

Final Report

Intersubband Quantum Cascade Infrared Laser Development Phase I

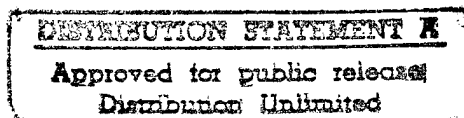
Contract No. DASG60-95-C-0038

Sponsored By
BMDO Innovative Science and Technology Office

Managed By
U.S. Army Space and Strategic Defense Command

19960717 019

prepared by
Quantum Epitaxial Designs, Inc.
Dr. Kenneth L. Bacher
(610) 861-6930



DTIC QUALITY INSPECTED 1

REPORT DOCUMENTATION PAGE			Form Approved OMB No. 0704-0188	
Public reporting burden for this collection of information is estimated to average 1 hour per response, including the time for reviewing instructions, searching existing data sources, gathering and maintaining the data needed, and completing and reviewing the collection of information. Send comments regarding this burden estimate or any other aspect of this collection of information, including suggestions for reducing this burden, to Washington Headquarters Services, Directorate for Information Operations and Reports, 1215 Jefferson Davis Highway, Suite 1204, Arlington, VA 22202-4302, and to the Office of Management and Budget, Paperwork Reduction Project (0704-0188), Washington, DC 20503.				
1. AGENCY USE ONLY (Leave blank)	2. REPORT DATE July 10, 1996	3. REPORT TYPE AND DATES COVERED Final Report, 6/95 - 7/96		
4. TITLE AND SUBTITLE Quantum Cascade Infrared Laser Development		5. FUNDING NUMBERS DASG60-95-C-0038		
6. AUTHOR(S) Dr. Kenneth L. Bacher				
7. PERFORMING ORGANIZATION NAME(S) AND ADDRESS(ES) Quantum Epitaxial Designs, Inc. 119 Technology Drive Bethlehem, PA 18015		8. PERFORMING ORGANIZATION REPORT NUMBER		
9. SPONSORING / MONITORING AGENCY NAME(S) AND ADDRESS(ES) U.S. Army Space and Strategic Defense Command P.O. Box 1500 Huntsville, AL 35807-3801		10. SPONSORING / MONITORING AGENCY REPORT NUMBER		
11. SUPPLEMENTARY NOTES				
12a. DISTRIBUTION / AVAILABILITY STATEMENT		12b. DISTRIBUTION CODE		
13. ABSTRACT (Maximum 200 words) <p>The objectives of this program were threefold: to reproduce the quantum cascade laser results from Bell Labs in a production environment, to demonstrate the quantum cascade laser at longer wavelengths, and to extend the technology to the GaAs/AlGaAs material system in order to make the lasers easier to produce. After characterization with 5-crystal x-ray diffraction and photoluminescence to verify the material quality, three laser wafers, with anticipated operating wavelengths near 4.5 microns and 8.5 microns, were grown, processed, and tested for this program. Although we were able to successfully grow the very thick lattice-matched layers necessary for these devices, no lasing or electroluminescence was observed from any of the samples. Another laser design was produced based on the reported quantum cascade laser structures, but utilizing GaAs and AlGaAs materials instead of InGaAs and InAlAs; however, because of the negative results with the InGaAs/InAlAs structure and additional design uncertainties for the AlGaAs materials, this structure was not grown.</p> <p>This report will discuss in detail the work that was performed on the contract, possible causes for the negative results, and conclusions drawn from the work.</p>				
14. SUBJECT TERMS IR Laser, Intersubband Laser, Molecular Beam Epitaxy, InGaAs, InAlAs, InP		15. NUMBER OF PAGES 10 + form 298		16. PRICE CODE
17. SECURITY CLASSIFICATION OF REPORT Unclassified	18. SECURITY CLASSIFICATION OF THIS PAGE Unclassified	19. SECURITY CLASSIFICATION OF ABSTRACT Unclassified	20. LIMITATION OF ABSTRACT SAR	

I Introduction:

Between the submission of the proposal and the commencement of work on this program, several papers from the people that initially developed the quantum cascade laser were published. These papers demonstrated improved designs, with increases in operating efficiency and variations in wavelength of the lasers.^{1,2} In order to optimize the chances of success, two separate designs were grown and processed. The design from reference 1 was chosen because it possessed a higher efficiency and, because it was based on Si doping rather than Sn, offered a more straight-forward chance for reproducing the Bell Labs results with our equipment. The design in reference 2 was chosen to give an output near 4.5 microns. Additionally, because of the more sensitive detection equipment available for this shorter wavelength, we hoped to get more information from the subthreshold luminescence from this design in the event that it did not lase. A structure was also designed to extend this work to the GaAs/AlGaAs materials system. This design was based on that for the 4.5 micron laser in reference 2, but involved some added difficulties due to the indirect band structure of AlGaAs for Al mole fractions greater than about 0.4. Because of this, it seemed fruitless to attempt to grow and process this design until positive results were obtained on the device designs which had already been demonstrated at Bell Labs.

II Work and Results:

The 8.5 micron design shown in Table 1 illustrates the complexity of these devices. All GaInAs and AlInAs layers are designed with indium mole fractions of 0.532 and 0.524 respectively so they will be lattice-matched to the InP substrate. If the compositions deviate too far from these values dislocations will be introduced during the 5.5 microns of material growth which will impede laser operation. By comparison, our typical production device thickness in this material system is less than 1 micron. Good surface morphology and the High Resolution X-Ray Diffraction (HRXRD) scans in Figure 1 verify that good lattice matching was accomplished for both laser samples, although slightly better for #8999.02 than for #8997.02. In the x-ray scans, the angular positions of the various peaks corresponds to the perpendicular lattice constant of the associated layer. Thus, the peak separation is indicative of the degree of lattice-matching. From the scans, one can see that the molar fractions of the layers in wafer #8997.02 are within 0.006 of the target values while those in wafer #8999.02 are within 0.004 of the target values. This data indicates that we were successful in controlling the GaInAs and AlInAs compositions to grow these thick lattice-matched structures in a production environment.

A photoluminescence spectrum from sample #8997.02 is shown in Figure 2. In this wavelength range, one would not see luminescence originating from either bulk AlInAs or bulk GaInAs layers. Quantization effects, however, will shift the luminescence wavelength of the thin GaInAs layers in the quantum well region of the device to shorter wavelengths, so they are evident in this range. Observation of room temperature photoluminescence from the quantum well region of the sample, especially considering the thickness of material above it in the structure, indicates efficient conduction- to valence-

band radiative recombination and thus good material quality. After characterization, these samples were sent to David Sarnoff Research Labs (DSRL) for processing and testing.

Sections of both samples were cleaved and processed into stripe lasers. An SiO_2 layer 150 nm thick was deposited and patterned to define the laser stripes of varying width. AuGeNiAu contacts were deposited on the epi side, and, after thinning to 100 microns, on the substrate side as well. Laser bars were cleaved with a cavity length of 1mm and the facets were coated to a reflectivity of 30%.

The lasers, mounted in TO-46 packages, were cooled to 78 K in a cryogenic Dewar for testing. For this wavelength range, a thermopile, lock-in amplifier, and chopper operating at 25 Hz were used to test for laser emission. Because the detector is a thermal detector rather than a photon detector, it operates at slower speeds, but should have a flat spectral response. As such, the measurement system was tested with a 1.5 micron CW laser. At 10 mW of laser output, the detector register 1.0 mV compared to the noise floor, with the laser off, of 0.003 mV. Thus, a signal-to-noise ratio of 1 should be attained with a CW power as low as 0.03 mW.

The measured I-V characteristics are in good agreement (within 10%) of the values expected from the Satori paper.¹ To attempt to observe lasing from these devices, four lasers were pulse tested with 100 nS pulses at a 2% duty cycle. Threshold was expected at a pulsed drive current near 440 mA; however, no lasing was observed even up to 1.8 A. Because of the low duty cycle, the output power necessary to achieve a unity S/N increased to 1.5 mW. Although this power level should easily have been achievable if the device had reached threshold, it is unlikely that subthreshold spontaneous emission would be observable with this detection system.

Because lasing was not observed in the samples, a second round of processing and testing was performed in an effort to more closely replicate the processing conditions from the Bell Labs paper. First, non-alloyed Ti/Au contacts were used instead of the alloyed AuGeNiAu contacts employed for the first processing run. Although the I-V characteristics of the tested lasers were in good agreement with that expected from the referenced work, there was concern that the alloying process might effect the properties of the laser. Second, a 20 micron wide ridge-waveguide structure was used instead of the stripe laser measured in the first go-around. Finally, since the Al_2O_3 facet coating becomes absorbing to radiation longer than 6.5 microns, no facet coatings were used in the next processing run.

This second processing run was performed simultaneously on sections from wafers #8999.02 ($\lambda \sim 8.5$ microns) and #9338.02 ($\lambda \sim 4.5$ microns). This second sample was based on the design in reference 2 as shown in Table 2. In that work, Sn was used as the n-type doping to enable very high doping of the contact layer. This doping is necessary not to reduce contact resistance, but to "decouple the guided laser mode from the surface plasmon mode propagating at the metal contact/semiconductor interface."³ Since Sn doping is incompatible with our production uses of the MBE reactor, it was impossible to use Sn for the growth of these layers and Si was substituted as the n-type doping source.

Four devices from wafer #8999.02 and three from wafer #9338.02 were examined at DSRL with the same result as before- no optical emission was observed. To verify that the problem did not lie with the measurement setup, the testing was repeated at Lucent Technologies. A 4.5 micron laser fabricated by Dr. Capasso's group (part of the original

team that demonstrated the quantum cascade laser) was used to verify that the measurement system was working correctly. A 2-3 μV noise floor for this setup corresponds to a minimum detectable power of ~ 10 pW. Under the testing conditions of 300 nS pulses at a 0.06% duty cycle, a minimum power of 17 nW is detectable. This should be low enough to see subthreshold spontaneous emission should the laser be close to threshold. Still no output was observable from any of the lasers even up to drive currents of 5 A.

III Problems:

The difficulty we have had reproducing the Bell Labs results and absence in the literature of other groups successfully demonstrating a quantum cascade laser indicates the extreme complexity of this device. A discussion with the person at Bell Labs responsible for the growth of the lasers indicated that there were no "tricks" to the growth, however, there are still several possible reasons for our inability to obtain working devices. One obvious potential difficulty concerns differences in machine calibration. Because the emission process is so dependent on the exact layer thicknesses in the quantum well/superlattice region, even very small errors could potentially cause large changes in device performance, or lack of operation at all. At QED, we use HRXRD measurement of calibration structures to calibrate layer compositions and thicknesses. We find this method produces very reproducible results which we feel also have a high degree of absolute accuracy. Nevertheless, it is possible that our layer thicknesses might not agree with those from an MBE reactor calibrated using other methods- even though these methods might also be very reproducible. In such circumstances it is very helpful to perform a cross-calibration wherein one calibration sample is analyzed by both facilities to determine if some calibration differences might exist. Since Bell Labs was not a collaborator in this project, however, this cross-calibration was not possible. Furthermore, since an indication of the layer thickness accuracy necessary to produce an operational device has not been published, it is difficult for us to determine whether our calibration methods are sufficient to produce an operational device.

Some design differences might have contributed to the unsuccessful results as well. At least in the case of the 4.5 micron lasers, there may have been differences caused by using Si instead of Sn for the n-type doping. It is very possible that the Si doping will not activate well at the very high $2 \times 10^{20} \text{ cm}^{-3}$ levels necessary for this structure. This would lead to increased loss for the lasing mode and possibly prevent lasing, but should not prevent the observation of spontaneous emission. Potentially, unintentional diffusion of the Sn doping in the Bell Labs growth might also have changed the structure in ways difficult to reproduce with Si doping. It is also probable that some ambiguities in the design, such as the method for performing the compositional grading between some layers in the structure resulted in a device that would not lase. Again, however, one would expect this to decrease the efficiency compared to a more optimized structure, but not eliminate the spontaneous emission altogether.

The first successful demonstration of the quantum cascade laser occurred only after a series of steps developing the technology to produce these devices.^{4,5,6} In addition

to allowing for optimization of the growth conditions, such as substrate temperatures and V/III ratios, on simpler structures, the development process necessarily resulted in a design which was optimized for the growth methodology employed at Bell Labs. Following a similar procedure, however, was not possible both because of the available time for the program and the available characterization resources. For example, the peak optical power output from the LEDs in reference 6 was only 6 nW, which is several orders of magnitude below the minimum detectable signals on the DSRL equipment. As a result it was difficult to gather information from our unsuccessful devices to use in improving later iterations.

IV Conclusion:

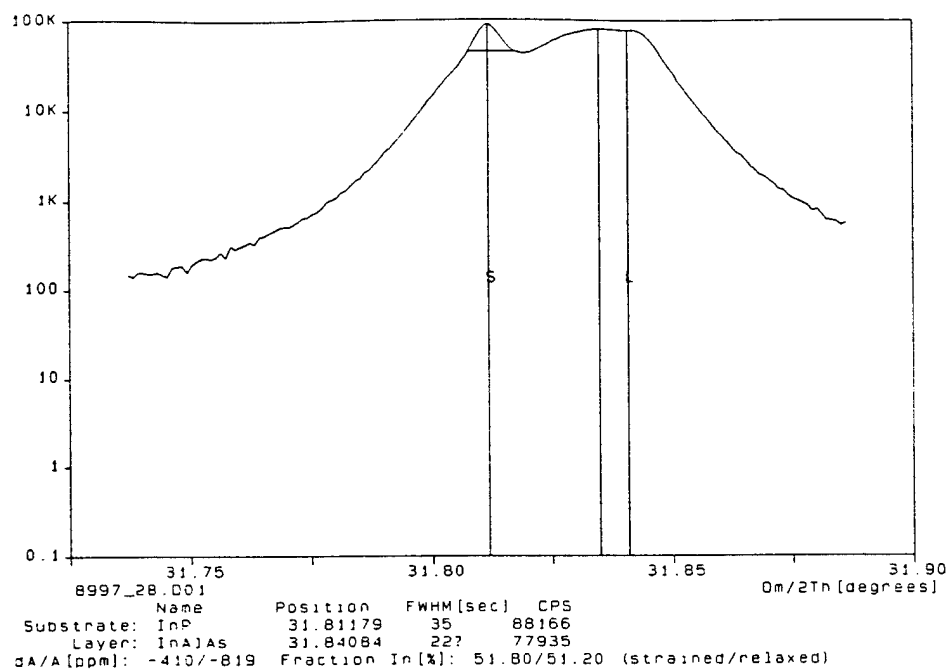
The complexities of the quantum cascade laser make it extremely difficult to reproduce based solely on the published designs without a more lengthy development process or closer collaboration with those who have demonstrated the device. More detailed discussion with the crystal growers, cross-calibration, and the ability to characterize material that resulted in working devices would allow problems with the growth of these devices to be identified and corrected. Similarly, processing and testing material that was known to yield working lasers would allow identification and correction of any processing problems. Without such a collaboration or technology transfer arrangement, however, a more involved development effort would be necessary to ensure successful demonstration of these devices. A program to first demonstrate the correct absorption properties of the such structures and allow optimization of the material growth would seem a realizable first step. Following this one could work on demonstrating spontaneous emission and then lasing. During this development process, access to a suitable measurement system for observing very small signal levels would be necessary to allow the optimization process to take place.

Table 1: Quantum cascade laser design for high efficiency output at 8.5 microns.

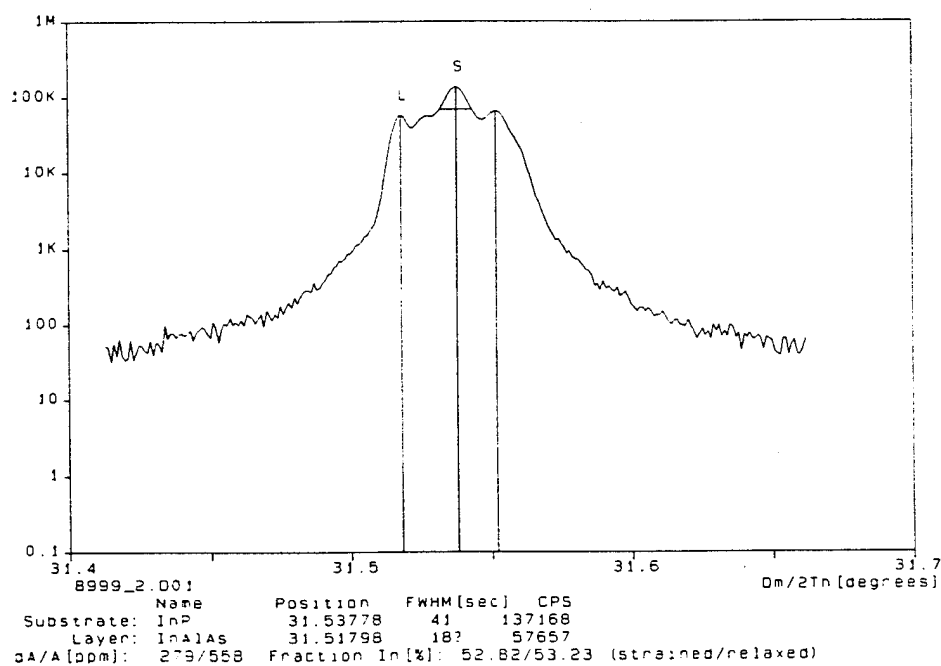
Layer	Thickness	Si Doping	Comments
InGaAs	6000 Å	$7 \times 10^{18} \text{ cm}^{-3}$	
AlGaAs=>InGaAs	300 Å	$5 \times 10^{17} \text{ cm}^{-3}$	Digital Grading
AlInAs	200 Å	$5 \times 10^{17} \text{ cm}^{-3}$	
AlInAs	12,000 Å	$3 \times 10^{17} \text{ cm}^{-3}$	
AlInAs	12,000 Å	$1.2 \times 10^{17} \text{ cm}^{-3}$	
AlInAs	100 Å	$1 \times 10^{18} \text{ cm}^{-3}$	
GaInAs=>AlInAs	400 Å	$2 \times 10^{17} \text{ cm}^{-3}$	Digital Grading
GaInAs	5000 Å	$6 \times 10^{16} \text{ cm}^{-3}$	
GaInAs	43 Å	-	\
AlInAs	10 Å	-	\
GaInAs	40 Å	$1.5 \times 10^{17} \text{ cm}^{-3}$	
AlInAs	8 Å	-	
GaInAs	42 Å	$1.5 \times 10^{17} \text{ cm}^{-3}$	
AlInAs	5 Å	-	
GaInAs	48 Å	-	\ Repeat
AlInAs	20 Å	-	/ 25X
GaInAs	58 Å	-	
AlInAs	20 Å	-	
GaInAs	75 Å	-	
AlInAs	20 Å	-	
GaInAs	35 Å	-	/
AlInAs	45 Å	-	/
GaInAs	7000 Å	$6 \times 10^{16} \text{ cm}^{-3}$	
(AlInAs) ₅ (GaInAs) ₅ => GaInAs	250 Å	$1.2 \times 10^{17} \text{ cm}^{-3}$	Digital Grading
InP	-	$5 \times 10^{17} \text{ cm}^{-3}$	

Table 2: Structure for 4.5 micron laser.

Layer	Thickness	Si Doping	Comments
GaInAs	100 Å	$2 \times 10^{20} \text{ cm}^{-3}$	
AlInAs => GaInAs	300 Å	$7 \times 10^{18} \text{ cm}^{-3}$	Digital Grading
AlInAs	7000 Å	$7 \times 10^{18} \text{ cm}^{-3}$	
AlInAs	6000 Å	$4 \times 10^{18} \text{ cm}^{-3}$	
AlInAs	10000 Å	$1.5 \times 10^{17} \text{ cm}^{-3}$	
GaInAs=>AlInAs	146 Å	$2 \times 10^{17} \text{ cm}^{-3}$	Digital Grading
GaInAs	3000 Å	$1 \times 10^{17} \text{ cm}^{-3}$	
AlInAs=>GaInAs	146 Å	$2 \times 10^{17} \text{ cm}^{-3}$	Digital Grading
AlInAs	65 Å	-	\
GaInAs	45 Å	-	\
AlInAs	28 Å	-	
GaInAs	36 Å	-	
AlInAs	30 Å	-	
GaInAs	21 Å	-	
AlInAs	21 Å	-	
GaInAs	21 Å	-	
AlInAs	21 Å	$3 \times 10^{17} \text{ cm}^{-3}$	\ Repeat
GaInAs	21 Å	$3 \times 10^{17} \text{ cm}^{-3}$	/ 25X
AlInAs	19 Å	$3 \times 10^{17} \text{ cm}^{-3}$	
GaInAs	16 Å	$3 \times 10^{17} \text{ cm}^{-3}$	
AlInAs	20 Å	$3 \times 10^{17} \text{ cm}^{-3}$	
GaInAs	17 Å	$3 \times 10^{17} \text{ cm}^{-3}$	
AlInAs	23 Å	$3 \times 10^{17} \text{ cm}^{-3}$	
GaInAs	13 Å	-	
AlInAs	27 Å	-	/
GaInAs	10 Å	-	/
GaInAs	3000 Å	$1 \times 10^{17} \text{ cm}^{-3}$	
AlInAs=>GaInAs	354 Å	$2 \times 10^{17} \text{ cm}^{-3}$	Digital Grading
AlInAs	7000 Å	$1.5 \times 10^{17} \text{ cm}^{-3}$	
InP	-	$5 \times 10^{17} \text{ cm}^{-3}$	



(a)



(b)

Figure 1: High resolution x-ray diffraction scans of wafers #8997.02 (a), and #8999.02 (b).

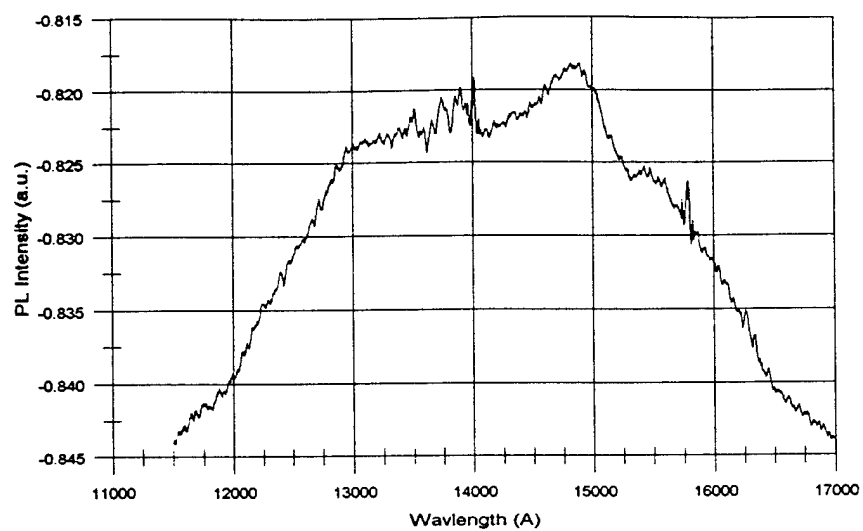


Figure 2: Photoluminescence from sample #8997.02 indicating band-to-band recombination in quantum well region.

References:

- ¹ Sirtori, et al., "Quantum cascade laser with plasmon-enhanced waveguide operating at 8.4 micron wavelength," Appl. Phys. Lett., 66 (24), pp. 3242-44, 1995.
- ² Faist, et al., "Vertical transition quantum cascade laser with Bragg confined excited state," Appl. Phys. Lett., 66 (5), pp. 538-40, 1995.
- ³ Faist, et al., "Vertical transition quantum cascade laser with Bragg confined excited state," Appl. Phys. Lett., 66 (5), pp. 539, 1995
- ⁴ Faist, et al., "Mid-infrared field-tunable intersubband electroluminescence at room temperature by photon-assisted tunneling in coupled-quantum wells," Appl. Phys. Lett., 64 (9), pp. 1144-46, 1994.
- ⁵ Faist, et al., "Narrowing of the intersubband electroluminescent spectrum in couple-quantum-well heterostructures," Appl. Phys. Lett., 65 (1), pp. 94-96, 1994.
- ⁶ Sirtori, et al., "Quantum cascade unipolar intersubband light emitting diodes in the 8-13 micron wavelength region," Appl. Phys. Lett., 66 (1), pp. 4-6, 1995.